Materials Today: Proceedings 93 (2023) 662–668

Contents lists available at ScienceDirect

Materials Today: Proceedings

journal homepage: www.elsevier.com/locate/matpr

Micromechanics of non-embedded spruce wood: Novel polishing and indentation protocol

Luis Zelaya-Lainez [a,*], Giuseppe Balduzzi [b], Olaf Lahayne [a], Markus Lukacevic [a], Christian Hellmich [a], Josef Füssl [a]

[a] Institute for Mechanics of Materials and Structures, Vienna University of Technology - TU Wien, 1040 Vienna, Austria
[b] Department of Civil Engineering and Architecture, University of Pavia, 27100 Pavia, Italy

ARTICLE INFO

Article history:
Available online 16 May 2023

Keywords:
Norway spruce
Nanoindentation
Cell wall
Reduced Modulus
Hardness
Biological preservation

ABSTRACT

Since the start of nanoindentation in wood, cell walls have been supported by epoxy resin during the microtoming of surfaces. However, wood embedding in epoxy resin was initially developed to harvest thin sections destined for transmission electron microscopy. In nanoindentation, embedding can affect the identified mechanical properties and might be difficult for modified wood samples. For this reason, we propose a protocol that does not involve resin within the wood specimen, uses a more robust miller to achieve surfaces with root means squared roughness of around 35 nm, and can exclude invalid edge indents through a novel evaluation procedure based on fitting 2D histograms with a linear combination of bi-variate lognormal probability density functions. We examined twelve samples of Norway spruce (*Picea abies*) late wood and their counterparts soaked with a biological preservation pretreatment. A nanoindentation protocol on every sample led to a mean reduced modulus and mean hardness of around 12 % and 26 %, respectively, lower than those found in the literature for embedded Norway spruce. These results agree well with previous results found for Loblolly pine (*Pinus taeda L.*) when comparing embedded and non-embedded specimens.

1. Introduction

[1] Wood is a biological material with a highly hierarchical organization in which the ultra-structural scale plays a crucial role in defining the macroscopic material properties [2]. Furthermore, the material's high porosity makes wood prone to impregnation with water and other chemical solvents or compounds. The first and foremost consequence of this property of wood is its hygroscopic behavior, deeply affecting its behavior [3,4]. This property is extensively exploited for several purposes, e.g., for wood preservation [5], consolidation of archaeological artifacts [6], and modification of wood's physical properties [7]. However, any change in chemical composition deeply affects the mechanical properties. For example, the consequences of impregnation with polyethylene glycol are well-known and deeply investigated, both from chemical and mechanical points of view [6]. Also, other preservative treatments significantly impacted the material's mechanical properties [8]. Still, most of the research on preservatives fittingly focuses on biological, toxicological, and environmental aspects [5], usually neglecting mechanics. On the contrary, impregnation effects on the mechanical properties are crucial for nanoindentation tests. Nanoindentation in wood started with the pioneering work of Wimmer et al. [9,10]. The standard experimental protocols allow embedding the sample in a material (usually an epoxy resin), filling all the pores [11,12]. This facilitates the preparation of the indentation surface, avoiding micro-cracks and other damages during milling and polishing [13]. However, the resin might chemically interact with the sample material, modifying its mechanical properties [14,15,16,17]. Unfortunately, chemical interaction is facilitated by (i) the high surface vs. volume ratio in wood samples and (ii) curing treatments that are required for the polymerization of the resin but can also promote other undesired reactions. The challenges of adequately choosing the embedding material and defining a non-invasive preparation of the wood sample have already been discussed. Anyway, the literature provides diverging conclusions, making the topic controversial. In their investigation on Norway spruce (*Picea abies*), Wagner et al. [12] concluded that

* Corresponding author.
E-mail address: Luis.Zelaya@tuwien.ac.at (L. Zelaya-Lainez).

https://doi.org/10.1016/j.matpr.2023.04.678
2214-7853/

"Using different embedding materials did not result in changes of the measured mechanical properties of the S2 cell wall layer. Also, the indentation of apparently non-embedded wood cell walls did not yield significantly different reduced modulus and hardness. Due to the lack of support of the cell walls by an embedding material during microtome cutting, the wood cell walls are frequently damaged, leading to higher variability of the obtained results.".

Conversely, considering a sample of Gray poplar (*Populus tremula* × *Populus alba*), Coste et al. [17] concluded: "that the use of resin embedding media to characterize plant cell walls at the nanoscale, although helpful to avoid damages, can lead to misleading analyses". Anyway, it has to be noticed that Wagner et al. [12] obtained a "non-embedded wood" sample by just avoiding vacuum treatment in the sample preparation procedure, resulting in "limited resin penetration into the cell lumina and in a substantial number of apparently non-embedded tracheids in the center of the specimen". Furthermore, [18,1,19] proposed innovative protocols that use resin and a microtome but with the samples not being in direct contact with resin. Meng et al. [1] wrapped a film between samples of Loblolly pine (*Pinus taeda L.*) or Red oak (*Quercus rubra*) and the resin. Compared to embedded specimens, they detected an increase in reduced elastic modulus when embedded of 14.2 % and 15.6 % for Loblolly pine and Red oak, respectively. Similarly, the hardness increased by 32 % and 11.3 %, respectively. Zelaya-Lainez et al. [20] proposed a novel milling polishing and indentation protocol for analyzing the micromechanical properties of non-embedded spruce wood. Preliminary results seem promising; however, several aspects still need to be appropriately addressed. This paper aims to further develop the sample preparation for nanoindentation. Our protocol makes it possible to use no resin at all to support the cell walls during microtoming or use a microtome at all. Moreover, we examine the usability of our method by comparing natural wood vs. wood that was treated with a commercial biological preservation solution. Last, we could identify the cell wall's reduced modulus and hardness values for both natural and treated wood with a novel procedure based on fitting 2D histograms with a linear combination of bi-variate lognormal Probability Density Functions (PDFs).

2. Materials and methods

2.1. Sample preparation

Twelve specimens of Norway spruce (*Picea abies*) with dimensions of approximately 20 mm × 20 mm × 40 mm in radial, tangential, and longitudinal directions ($r \times t \times l$) were harvested from various boards using a panel circular saw with a 2.5 mm wide blade (Holzprofi Pichlmann, Austria). Subsequently, each cuboid was cut into halves resulting in two similar samples per specimen (twenty-four in total) by means of a table saw with a 0.5 mm wide blade (Proxxon, Germany), sketched in Fig. 1(a,b). Twelve sample halves were stored for one year in a climate chamber (Binder, Germany) set at 21 degrees centigrade and 35 % relative humidity. Their twelve counterpart sample halves were introduced into a commercially available biological preservation treatment solution for six months. The weights of each immersed sample were monitored monthly by means of a precision balance (model PGH403-S from Mettler-Toledo Inc., Switzerland) until no mass change was recorded, and the samples were regarded as fully saturated with the treatment. The excess moisture was removed with a paper towel, and the samples were later stored in the before-described climate chamber at 21 degrees centigrade and 35 % relative humidity for six months. Subsequently, the 24 samples were attached to microscope glass slides with a thickness of 1.7 mm through a 2-component epoxy resin (Struers, Denmark). The resin was used only to secure the specimen in place. Thus, the resin was never in contact with the sample's surface. Nevertheless, other holding mechanisms without resin could also be employed. The 1.7 mm thick glass benefits the polishing protocol by reducing vibrations that may be introduced during the process of material removal. The surfaces orthogonal to the samples' longitudinal axis were milled by a Leica SM2500 heavy-duty sectioning system and the Leica SP2600 ultramiller (Leica Biosystems, Germany) with a diamond blade rotating at 1500 rpm, sketched in Fig. 1(c). A premiller was first used to remove most of the zone affected by the sawing protocol. The surface was further polished with a finishing miller until a mirror-like finish. The result-finishes of the sample surfaces attained by the milling protocol were observed by means of a Zeiss AxioImager light microscopy (Carl Zeiss, Germany). Photographs were recorded by means of an AxioCam MRc5 (Carl Zeiss, Germany), as seen in Fig. 2. Thereafter, the samples were stored in the climate chamber at 21 degrees centigrade and 35 % relative humidity until further tested.

2.2. Nanoindentation

The roughness of each sample was measured by means of scanning probe microscopy (SPM) in areas measuring 20 by 20 μm^2. An exemplary topological scan is given in Fig. 2(b). The roughness can be quantified as the root mean squared (RMS) roughness (R_q) and computed as:

$$R_q = \sqrt{\frac{\int_0^{l_1}\int_0^{l_2}\left[z(x,y)-\bar{z}\right]^2 dxdy}{l_1 l_2}}, \tag{1}$$

where z is the profile height given by the coordinates x and y. $\bar{z}$ is the average profile height and $l_1 = l_2$ = 20 μm.

2.3. Length scales

With nanoindentation protocols, material properties at nano- and micro-scales can be identified. However, the intended length scale must be carefully defined to correctly characterize the elastic and hardness properties of the material system we intend to investigate. The relationship among the relevant length scales can be obtained from the classical separation of scales [21] as follows:

$$d \ll l_{RVE} \ll \mathscr{L} \tag{2}$$

where d is the characteristic length of the microheterogeneity and is a lot smaller than the characteristic length of the representative volume element (RVE), which is a lot smaller than the structural length scale $\mathscr{L}$.

According to Königsberger et al. [22], we can relate the arguments from Drugan and Willis [23] on d to l_{RVE}, and combine them with results from ultrasonic campaigns [24] to obtain a quantitative relationship from Equation (2), as follows.

$$(2\cdots 3)d \le l_{RVE} \le \mathscr{L}/10 \tag{3}$$

Furthermore, according to Königsberger et al. [22], in Equation (3), $\mathscr{L}$ is approximately related to the characteristic length of the Berkovich indenter tip projected area A_c. This evolves into the relationship between the size of the RVE and the projected area, and this is computed as follows:

$$(2\cdots 3)d \le l_{RVE} \le \sqrt{A_c}/10 \tag{4}$$

The projected area of a perfect Berkovich tip is related to the contact depth h_c as follows:

$$A_c = 24.5h_c^2 \tag{5}$$

Equations (4) and (5) allow us to link the characteristic length of the microheterogeneity, the contact depth, and the RVE size as follows:

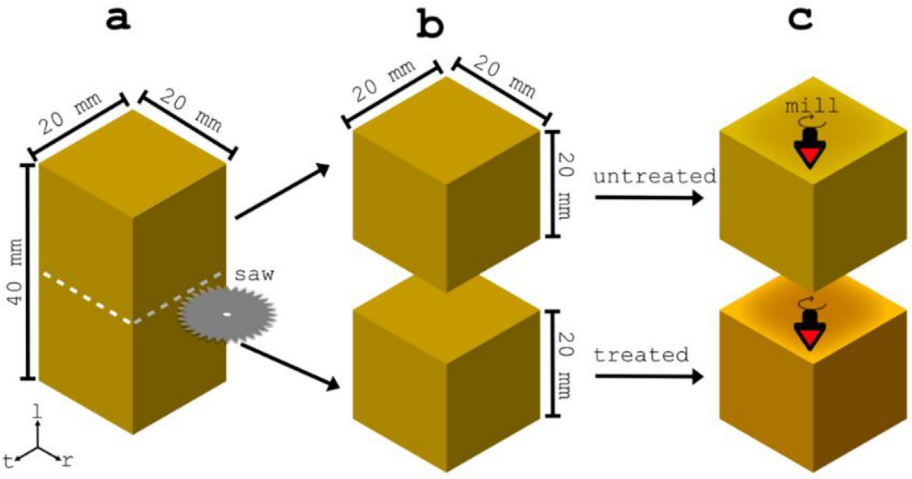

Fig. 1. Sample preparation (a) cuboid saw into two similar halves (b) one half was left untreated, and its counterpart was treated with a biological preservation treatment (c) the surface of both halves was polished by means of an ultramiller.

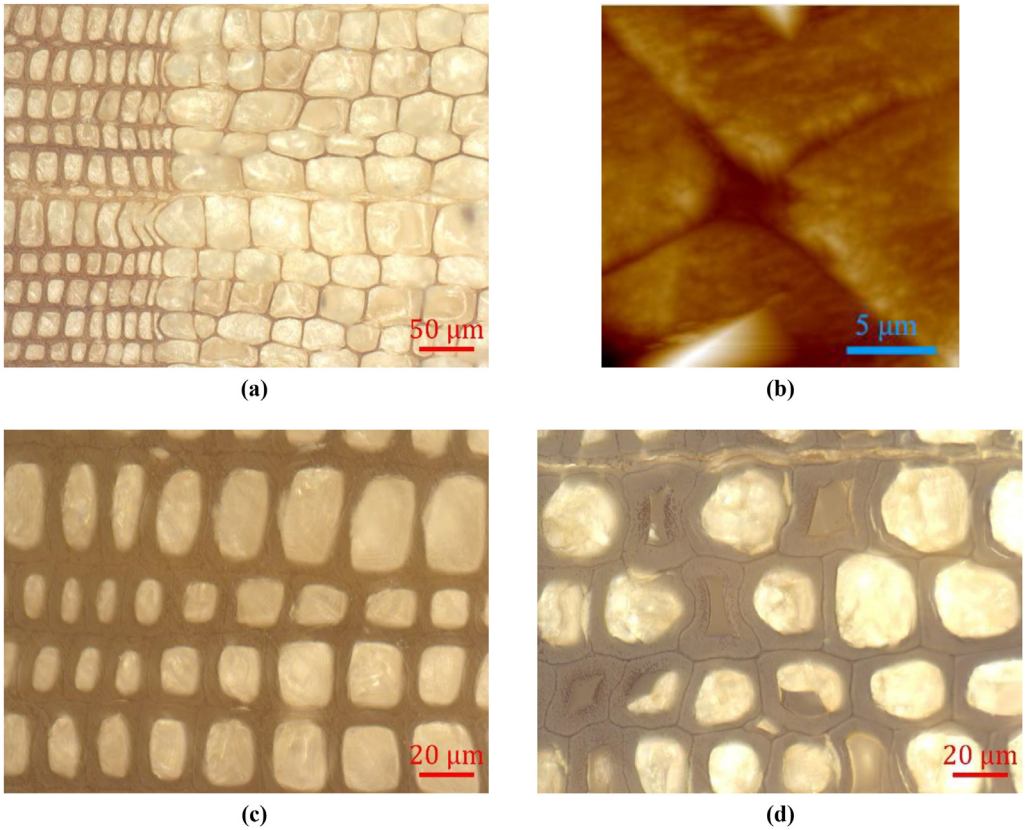

Fig. 2. Sample imaging: (a) Light microscopy image (100-fold magnification) of the polished surface of untreated spruce wood. The right part is the early wood and the left part is the late wood. (b) Topographic image (20x20 µm^2) of surface measured through SPM with a roughness of approximately 35 nm. (c) Light microscopy image (500-fold magnification) of sample U4 (untreated) late wood (d) Light microscopy image (500-fold magnification) of sample M7 (treated) late wood.

$$l_{RVE} \leq \frac{h_c\sqrt{24.5}}{10} \approx h_c/2 \tag{6}$$

$$d \leq \frac{h_c}{(4\cdots 6)} \tag{7}$$

The RVE size has to be related to the maximum surface roughness that permits physically reasonable measurements, as follows:

$$R_q \leq \frac{h_c}{2} \approx l_{RVE} \tag{8}$$

Furthermore, this goes by the observation made by Donnelly et al. [25], who gave h_c/R_q minimum ratios ranging from 1.7 to 2.8. We obtained h_c of approximately 270 nm and R_q of roughly 35 nm. Therefore, fulfilling the indentation depth and roughness requirement ratio by at least seven times.

The nanoindenter probe half-space $\mathscr{D}$ defined by Königsberger et al. [22], is considered to be at least ten times the indentation

depth. Considering our indentation depth measures approximately 270 nm means $\mathscr{D}$ is contemplated to be about 2.7μ m. Through light microscope images like the one in Fig. 2, we conclude that only indents far away from any lumen, crack, or other imperfection by a minimum of 2.7μ m can be considered. It is safe to say that most of the indents that fall in the earlywood section will not fulfill this criterion. Thus, just the latewood was considered for the indentation protocol.

2.4. Protocol of indents

Two locations at latewood sections of each sample (natural and treated) were indented in 10 × 10 grids by means of a Triboindenter with an attached three-sided pyramid Berkovich diamond tip (Hysitron, USA). All the 4800 indents were performed in a displacement-controlled fashion with a maximum indentation depth (h_{max}) of 300 nm. The indents were analyzed according to the Oliver and Pharr method [26].

2.5. Data analysis

Indentation modulus of the material E_r and indentation hardness Hhave been extracted from the indentation procedure output and collected in two separate sets according to the treatment of wood (unmodified and modified wood data are labeled with superscript *unmod* and *mod*, respectively). The data distribution for each sample has been qualitatively compared, aiming at excluding systematic errors on single samples. If the data distribution for a specific sample looked substantially different with respect to the others, the data have been discharged, and the polishing and the indentation protocol on the sample are repeated as described in Section 2.1. Furthermore, if an experiment provides a clearly invalid result ($E_r > 50GPa$ or $H > 1.2GPa$), both indentation modulus E_r and indentation hardness H have been deleted from the database. As a result of this procedure, 2400 (0 invalid results) and 2396 (4 invalid results) values constitute the datasets for unmodified and modified latewood, respectively.

Table 1 reports the results of the preliminary statistical analysis of the measured indentation modulus E_r and hardness H. The preservative treatment slightly increases the stiffness of the material ($mean\left(E_r^{mod}\right) > mean\left(E_r^{unmod}\right)$ and $max\left(E_r^{mod}\right) > max\left(E_r^{unmod}\right)$), but also the data dispersion ($std\left(E_r^{mod}\right) > std\left(E_r^{unmod}\right)$). Contrarily, the mean value of the hardness decreases for treated wood ($mean\left(H^{mod}\right) < mean\left(H^{unmod}\right)$), but both the maximal value and the standard deviation significantly increase ($max\left(H^{mod}\right) > max\left(H^{unmod}\right)$ and $std\left(H^{mod}\right) > std\left(H^{unmod}\right)$).

The lower bound of the 99.7% confidence interval ($mean(E_r) - 3std(E_r)$) turns out to be negative for all the considered data sets. Conversely, indentation modulus E_r and hardness H are positive by definition. This contradiction indicates that Gaussian PDF does not correctly represent the stochastic distribution of the data we are considering, despite being widely used in literature for similar problems [27]. We decided to describe the distribution of data using a linear combination of lognormal PDFs, aiming at improving the consistency of the statistical model with the physics of the material.

A well-established approach for data analysis consists of treating stiffness and hardness data separately, fitting separate histograms with linear combinations of PDFs representing the different phases constituting the analyzed material [28,29]. However, the standard approach applied to the specific problem under investigation produces controversial results: Fig. 3(b) and 3(c) depict E_r and H histograms for unmodified latewood. On the one hand, three different phases compose the material (see Table 2). On the other hand, while in Fig. 3(b) it is possible to qualitatively recognize two local maxima, Fig. 3(c) allows only one identification. The overlapping of populations with similar statistical properties (as sketched in Fig. 3(a)) can justify such behavior in E_r and H histograms.

Aiming at bypassing the problem mentioned above, we run data analysis interpolating 2D distribution of data (E_r, H) with a linear combination of three bi-variate lognormal PDFs

$$h(E,H) = \sum_{i=1}^{3} \times \frac{c_i}{2\pi\sigma_{Ei}\sigma_{Hi}\sqrt{1-\rho_i^2}} \exp\left(\frac{-1}{2(1-\rho_i)^2}\left(\frac{(\ln(E)-\mu_{Ei})^2}{\sigma_{Ei}^2} + \frac{(\ln(H)-\mu_{Hi})^2}{\sigma_{Hi}^2} - 2\rho_i \frac{\ln(E)-\mu_{Ei}}{\sigma_{Ei}} \frac{\ln(H)-\mu_{Hi}}{\sigma_{hi}}\right)\right) \tag{9}$$

where, for every, i^{th} lognormal distribution, μ_{ji} and σ_{ji} for $j = E_r, H$ are the mean and standard deviation of the variable's natural logarithm, respectively, $\rho_i$are the correlation coefficients, and the weights of the PDF c_i have to satisfy the following conditions: $0 < c_i < 1$ and $\sum_{i=1}^{3} c_i = 1$. From a practical point of view, such a choice is equivalent to considering normal PDFs of the variables $\ln(E)$ and $\ln(H)$. Thereafter, the 2D histogram of the new variable was created using a mesh of 100 × 100 bins. Finally, we assumed N = 3 on the basis of a simple physical consideration: In clear wood, we are able to distinguish at least three phases with significantly different mechanical properties, as indicated in Table 2.

Surface fitting, i.e., the searching of optimal parameters in Equation (9) has been done using the function fit available in MATLAB. The function requires bounding of the parameter values, allowing to enforce constraints in the optimization problem. For the problem we are analyzing, the parameters have been bounded as follows: $0 < c_i < 1$, $-1 < \rho_i < 1, \min(\ln(j)) < \mu_{ji} < \max(\ln(j))$, $0 < \sigma_{ji} < (\max(\ln(j)) - \min(\ln(j)))/6$. The advantage of this operation is twofold. On the one hand, we limit the size of the space where the algorithm has to search for the solution, simplifying the problem and reducing the computational cost. On the other hand, the option allows the implementation of physical and mathematical bounds, like limitations of the weight coefficients. The MATLAB function is available in the supplementary material. Among the solutions we found, we choose the one with the lowest RMS error (RMSE).

3. Results & discussion

Table 2 reports the properties of phases constituting the latewood. Fig. 5 reports the 2D fitting for modified and unmodified wood.

Table 1
Raw data statistics of indentation modulus E_r and hardness H for unmodified and modified latewood.

	unmod	*mod*		*unmod*	*mod*
$mean(E_r)$ [GPa]	10.610	10.763	$mean(H)$ [GPa]	0.332	0.261
$max(E_r)$ [GPa]	28.342	36.339	$max(H)$ [GPa]	1.048	1.217
$std(E_r)$ [GPa]	5.156	6.559	$std(H)$ [GPa]	0.124	0.169
$mean(E_r) - 3std(E_r)$ [GPa]	−4.858	−8.914	$mean(H) - 3std(H)$ [GPa]	−0.040	−0.246

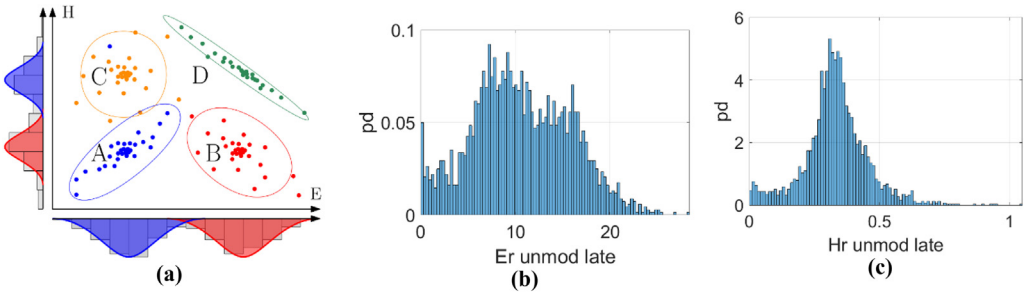

Fig. 3. Comparison of standard data analysis method and the proposed one: (a) Sketch of typical data analysis (histograms on the axis) and approach presented in this paper (2D plot). (b) Histogram of the indentation modulus E_r for unmodified wood. (c) Histogram of the indentation hardness H for unmodified wood.

Table 2
Mechanical properties of phases constituting latewood. The tracheid volume fraction has been estimated by analyzing Fig. 2. Indentation stiffness and hardness E_{ref} and H_{ref} have been obatined from [11]. Ratios between embedded and non-embedded material have been taken from [1], referring to Loblolly pine.

	phase	vol frac [%]	PDF #	c_i	E_{ref}[GPa]	Emb/non-emb ratio	E_{red} [GPa]	E_r[GPa]
					H_{ref}[GPa]		H_{red} [GPa]	H[GPa]
Unmodified wood	tracheid lumen	40–50	1	0.51	0.00	–	–	–
					0.00	–	–	–
	S2 layer	10–25	2	0.25	17.1	1.14	15.0	15.1
					0.47	1.32	0.356	0.348
	CWC	25–50	3	0.23	–	–	–	8.8
					–	–	–	0.32
Modified wood	tracheid lumen	40–50	1	0.46	0.00	–	–	1.29
					0.00	–	–	0.026
	S2 layer	10–25	2	0.08	17.1	1.14	15.0	14.4
					0.47	1.32	0.356	0.234
	CWC	25–50	3	0.46	–	–	–	9.60
					–	–	–	0.234

The area of tracheid lumens in latewood has been estimated on light microscope images, such as Fig. 2. The obtained estimation of tracheid volume fractions ranges between 40 and 50 %, with values at the upper limit identified at the transition zone to the early wood. Conversely, the region that we define cell wall compound (CWC) -i.e., primary wall, middle lamella, and cell wall in the neighborhood of lumen- should occupy approximately 25 to 50 % of the indentation surface, according to estimates provided in Section 2.3 and assuming a cell wall thickness of 7μm (see Fig. 2(c) and 2(d)). Consequently, the indents of the properly called S2 layer are expected to be 10 to 25 % of the results, as reported in Table 2.

Fig. 3(b) and 3(c) show the 1D histograms of indentation stiffness and hardness of latewood, considered separately. Based on these histograms, no distinct mechanical phases can be identified. A reasonable justification for the obtained results is depicted in Fig. 4: The indenter tip enters the tracheid lumen until the indenter edge touches the tracheid wall, leading to detect a force that, however, is not the consequence of the assumed experimental mechanism. Consequently, the results obtained from these indents are invalid and must not be considered in the analysis. The correct identification of spurious data represented an insurmountable obstacle in data analysis based on 1D histograms. Conversely, the analysis described in Section 2.5 allows identifying a population of data whose characteristics (PDF weight, mode, and standard deviation) can be associated with invalid data produced by improper contact of the indenter with the sample surface.

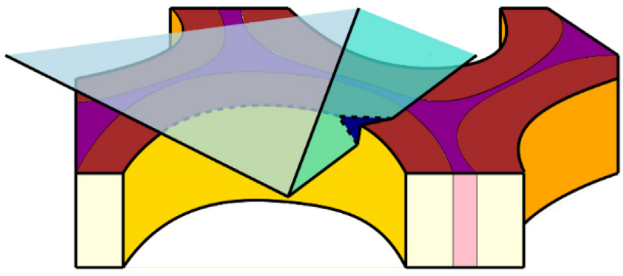

Fig. 4. Representation of the assumed invalid indentation mechanism.

Indeed, in Fig. 5 (a), PDF #1 weighs 0.51, and it is characterized by a low stiffness and hardness (6.04 and 0.234 GPa, respectively), which is far away from values reported in the literature for spruce wood) and a large standard deviation. Furthermore, it largely overlaps with both PDFs #2 and #3. PDFs #2 and #3 have similar weights (0.25 and 0.23, respectively). Consequently, they can be interpreted as the results of indentation into the S2 layer and CWC since these two phases may have similar volume fractions. PDF #2 provides the highest indentation stiffness and hardness (15.1 and 0.348 GPa, respectively) and also the highest correlation. Therefore, it can be associated with the indentation of the S2 layer.

Fig. 2(d) shows that in treated wood, the tracheid lumens are filled by residuals of preservative liquid. Consistently, in Fig. 5(b) PDF #1 has a weight of 0.46, the characteristic stiffness and hardness are one order of magnitude smaller than the one of the other phases (1.29 and 0.026 GPa, respectively), indicating that the indentation procedure correctly detects the solid phase in lumens and the filling material is exceptionally soft compared to other phases.

PDFs #2 and #3 have a weight of 0.08 and 0.46, respectively. In particular, PDF #2 again presents the highest characteristic values (14.4 and 0.23 GPa, respectively) and correlation. Therefore, it can be associated with the indentation of the S2 layer. Different weights between unmodified and modified latewood may result from greater noise in modified wood data.

Gindl et al. [11] documented an indentation modulus E_{ref} and hardness H_{ref} of 17.1 GPa and 0.47 GPa, respectively, for embedded

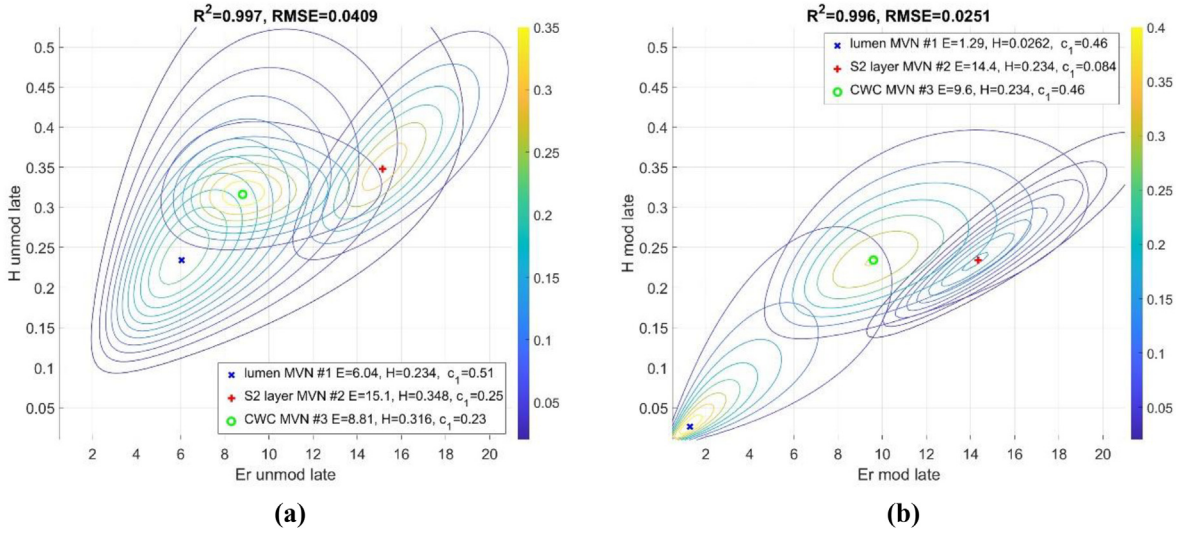

Fig. 5. 2D fitting of the indentation results, done with three bi-variate lognormal PDFs on (a) the natural samples (unmod late), (b) treated samples (mod late).

Norway spruce (*Picea abies*). The latter information is available in Table 2. Meng et al. [1] noted a 14% decrease in indentation modulus and a 32% decrease in hardness when comparing embedded Loblolly pine (*Pinus taeda L.*) samples to their non-embedded counterparts. We hypothesized that a similar reduction would be observed in the embedded and non-embedded samples of Norway spruce (*Picea abies*). Consequently, we introduced the variables "reduced" indentation modulus $E_{red}$and hardness H_{red}, which account for the absence of embedding material in the tracheid lumens. These reduced values are derived by dividing the reference values E_{ref} and H_{ref} by the embedded-to-non-embedded ratios obtained from [1].

Table 2 displays our experimental results, indicating that the E_r value of 15.1 GPa we obtained for the S2 layer aligns closely with the reduced value E_{red}, with a relative difference of just 0.7%. However, our H value of 0.348 GPa for the S2 layer exhibits a 2.2% difference when compared to the H_{red} value. Ultimately, our E_r and H values are 12% and 26% lower, respectively, than the reference values of indentation modulus E_{ref} and hardness H_{ref} found in the literature for embedded Norway spruce [11].

4. Conclusions

This paper presents a protocol that does not involve resin within the wood specimen and uses a more robust miller to achieve surfaces with RMS roughness of around 35 nm. Twelve pieces of Norway spruce (*Picea abies*) and their counterparts treated with a biological preservation pretreatment have been analyzed. After repeating the nanoindentation protocol 100 times on late wood of every sample, we determined indentation stiffness and hardness with a novel procedure based on fitting 2D histograms with a linear combination of bi-variate lognormal PDFs. Data analysis accounted for the presence of three phases and loose mathematical constraints of parameters only. However, the resulting PDFs can be easily associated with specific material phases, with high accuracy of all the parameters. We obtained indentation modulus and hardness values, which are around 12 % and 26% respectively lower than the ones found in the literature for embedded Norway spruce. The results on E_r agree well with previous results found for Loblolly pine or Red oak when comparing embedded and non-embedded specimens. Preparation protocols, indentation protocols, and reliable evaluation algorithms for non-embedded samples are necessary to test certain modified wood samples reliably.

CRediT authorship contribution statement

Luis Zelaya-Lainez: Conceptualization, Investigation, Data curation, Writing – original draft. **Giuseppe Balduzzi:** Investigation, Data curation, Writing – original draft. **Olaf Lahayne:** Investigation. **Markus Lukacevic:** Investigation, Writing – review & editing. **Christian Hellmich:** Conceptualization, Investigation. **Josef Füssl:** Conceptualization, Funding acquisition, Resources, Writing – review & editing.

Data availability

Data will be made available on request.

Declaration of Competing Interest

The authors declare that they have no known competing financial interests or personal relationships that could have appeared to influence the work reported in this paper.

Acknowledgments

The authors gratefully acknowledged the funding from the Austrian Science Fund (FWF) through the START grant Y1093 "Virtual Wood Labs" and SFB F77 "Advanced Computational Design".

References

[1] Y. Meng, S. Wang, Z. Cai, T. M. Young, G. Du and Y. Li, "A Novel Sample Preparation Method to Avoid Influence of Embedding Medium during Nano-Indentation," *Applied Physics A,* vol. 110, p. 361–369, 2 2013.
[2] K. Hofstetter, C. Hellmich and J. Eberhardsteiner, "Development and Experimental Validation of a Continuum Micromechanics Model for the Elasticity of Wood," *European Journal of Mechanics - A/Solids,* vol. 24, p. 1030–1053, 1 11 2005.
[3] M. Autengruber, M. Lukacevic, J. Füssl, Finite-element-based moisture transport model for wood including free water above the fiber saturation point, Int. J. Heat Mass Transf. 161 (1 11 2020.).
[4] H. J. Blaß and C. Sandhaas, "Timber Engineering - Principles for Design," 2017. [Online]. Available: https://publikationen.bibliothek.kit.edu/1000069616.
[5] A. Barbero-López, J. Akkanen, R. Lappalainen, S. Peräniemi, A. Haapala, Bio-based wood preservatives: their efficiency, leaching and ecotoxicity compared to a commercial wood preservative, Sci. Total Environ. 753 (20 1 2021.).

[6] E. Hocker, G. Almkvist and M. Sahlstedt, "The Vasa Experience with Polyethylene Glycol: A Conservator's Perspective," *Journal of Cultural Heritage,* vol. 13, no. 3, Supplement, pp. S175-S182, 1 9 2012.
[7] Y. Li, Q. Fu, S. Yu, M. Yan and L. Berglund, "Optically Transparent Wood from a Nanoporous Cellulosic Template: Combining Functional and Structural Performance," *Biomacromolecules,* vol. 17, p. 1358–1364, 11 4 2016.
[8] L. Sommerauer, M.-F. Thevenon, A. Petutschnigg and G. Tondi, "Effect of Hardening Parameters of Wood Preservatives Based on Tannin Copolymers," *Holzforschung,* vol. 73, p. 457–467, 1 5 2019.
[9] R. Wimmer, B. N. Lucas, W. C. Oliver and T. Y. Tsui, "Longitudinal Hardness and Young's Modulus of Spruce Tracheid Secondary Walls Using Nanoindentation Technique," *Wood Science and Technology,* vol. 31, p. 131–141, 1 4 1997.
[10] R. Wimmer and B. N. Lucas, "Comparing Mechanical Properties of Secondary Wall and Cell Corner Middle Lamella in Spruce Wood," *IAWA Journal,* vol. 18, p. 77–88, 1 1 1997.
[11] W. Gindl, H. S. Gupta, T. Schöberl, H. C. Lichtenegger and P. Fratzl, "Mechanical Properties of Spruce Wood Cell Walls by Nanoindentation," *Applied Physics A,* vol. 79, p. 2069–2073, 1 12 2004.
[12] L. Wagner, T. K. Bader and K. de Borst, "Nanoindentation of Wood Cell Walls: Effects of Sample Preparation and Indentation Protocol," *Journal of Materials Science,* vol. 49, p. 94–102, 1 1 2014.
[13] A. R. Spurr, "A Low-Viscosity Epoxy Resin Embedding Medium for Electron Microscopy," *Journal of Ultrastructure Research,* vol. 26, p. 31–43, 1 1 1969.
[14] J. Konnerth, D. Harper, S.-H. Lee, T. G. Rials and W. Gindl, "Adhesive Penetration of Wood Cell Walls Investigated by Scanning Thermal Microscopy (SThM)," *hfsg,* vol. 62, p. 91–98, 1 1 2008.
[15] J. E. Jakes and D. S. Stone, "Best Practices for Quasistatic Berkovich Nanoindentation of Wood Cell Walls," *Forests,* vol. 12, no. 12, p. 1696, 12 2021.
[16] J.-W. Kim, D.P. Harper, A.M. Taylor, Technical note: effect of epoxy embedment on micromechanical properties of brown-rot-decayed wood cell walls assessed with nanoindentation, Wood Fiber Sci. 13 (1) (2012) 103–107.
[17] R. Coste, M. Soliman, N.B. Bercu, S. Potiron, K. Lasri, V. Aguié-Béghin, L. Tetard, B. Chabbert, M. Molinari, Unveiling the impact of embedding resins on the physicochemical traits of wood cell walls with subcellular functional probing, Compos. Sci. Technol. 201 (5 1 2021.).
[18] J. E. Jakes, C. R. Frihart, J. F. Beecher, R. J. Moon and D. S. Stone, "Experimental Method to Account for Structural Compliance in Nanoindentation Measurements," *Journal of Materials Research,* vol. 23, p. 1113–1127, 4 2008.
[19] T. Keplinger, J. Konnerth, V. Aguié-Béghin, M. Rüggeberg, N. Gierlinger, I. Burgert, A zoom into the nanoscale texture of secondary cell walls, Plant Methods 10 (10 1 2014) 1.
[20] L. Zelaya-Lainez, O. Lahayne, G. Balduzzi and C. Hellmich, Micromechanics of Non-Embedded Spruce Wood: Novel Polishing and Indentation Protocol, University of West Bohemia, 2019
[21] A. Zaoui, "Continuum Micromechanics: Survey," *Journal of Engineering Mechanics,* vol. 128, p. 808–816, 1 8 2002.
[22] M. Königsberger, L. Zelaya-Lainez, O. Lahayne, B. L. A. Pichler and C. Hellmich, "Nanoindentation-Probed Oliver-Pharr Half-Spaces in Alkali-Activated Slag-Fly Ash Pastes: Multimethod Identification of Microelasticity and Hardness," *Mechanics of Advanced Materials and Structures,* vol. 29, p. 4878–4889, 26 10 2022.
[23] W. J. Drugan and J. R. Willis, "A Micromechanics-Based Nonlocal Constitutive Equation and Estimates of Representative Volume Element Size for Elastic Composites," *Journal of the Mechanics and Physics of Solids,* vol. 44, p. 497–524, 1 4 1996.
[24] C. Kohlhauser and C. Hellmich, "Ultrasonic Contact Pulse Transmission for Elastic Wave Velocity and Stiffness Determination: Influence of Specimen Geometry and Porosity," *Engineering Structures,* vol. 47, p. 115–133, 1 2 2013.
[25] E. Donnelly, S.P. Baker, A.L. Boskey, M.C.H. van der Meulen, Effects of surface roughness and maximum load on the mechanical properties of cancellous bone measured by nanoindentation, J. Biomed. Mater. Res. A 77A (2006) 426–435.
[26] W. C. Oliver and G. M. Pharr, "An Improved Technique for Determining Hardness and Elastic Modulus Using Load and Displacement Sensing Indentation Experiments," *Journal of Materials Research,* vol. 7, p. 1564–1583, 6 1992.
[27] G. Kandler, J. Füssl, E. Serrano, J. Eberhardsteiner, Effective stiffness prediction of GLT beams based on stiffness distributions of individual lamellas, Wood Sci. Technol. 49 (4) (2015) 1101–11021.
[28] O. Lahayne, L. Zelaya-Lainez, T. Buchner, J. Eberhardsteiner and J. Füssl, "Influence of Nanoadditives on the Young's Modulus of Cement," *Materials Today: Proceedings,* vol. 62, p. 2488–2494, 1 1 2022.
[29] P. Dohnalík, B.L.A. Pichler, L. Zelaya-Lainez, O. Lahayne, G. Richard, C. Hellmich, Micromechanics of dental cement paste, J. Mech. Behav. Biomed. Mater. 124 (1 12 2021).